A Tomographic Multiview-Multistatic Ultrasound System for Biomedical Imaging Applications

S. Franceschini[a], M. Ambrosanio[b], F. Baselice[c] and V. Pascazio[d]
Department of Engineering, University of Naples Parthenope, Naples, Italy
{*stefano.franceschini, michele.ambrosanio, fabio.baselice, vito.pascazio*}*@uniparthenope.it*

Keywords: Ultrasound Systems, Tomographic Imaging, MIMO Systems, Biomedical Imaging, Object Detection.

Abstract: Medical imaging is a paramount concern in modern society. Thus, there is an increasing interest and attention to new imaging modalities which can support standard exams and/or replace them in diseases diagnosis. In this framework, ultrasound tomography could have an important role for some biomedical applications, such as for breast cancer imaging, since it would allow to overcome some limitations related to standard ultrasound exams which are operator-dependent and usually are not based on a coherent processing, reducing the reconstruction performance considerably. To this aim, in this article a preliminary air-based ultrasound tomographic imaging system is described and tested. The prototype was designed, built and tested at the University of Naples Parthenope with the aim of providing some interesting data sets for testing and comparison of imaging algorithms in a laboratory-controlled environment, which represents a mandatory step before moving to the realistic case of a water-matched device.

1 MOTIVATION

Ultrasound tomography (UT) is an interesting non-destructive imaging modality which exploits mechanical waves to provide quantitative as well as qualitative maps of the objects located in an investigated domain which is usually inaccessible, such as in some industrial and biomedical applications (Abdollahi et al., 2019; Alqadah, 2016; Mojabi and LoVetri, 2017).

In clinical practice, Ultrasound (US) scanners are widely adopted due to the low cost, the easy management and the safety for the patient. Their main limitation is that a subjective analysis is allowed, as produced results are operator-dependent. This is also the reason why the examination is conducted by the doctor himself instead by a technician, as in magnetic resonance imaging (MRI) or computerized tomography (CT) systems. UT approach has the intent of overcoming this issue, being a tomographic, operator-independent acquisition system that makes use of acoustic waves. Moreover, its peculiarity of implementing coherent processing allows to obtain data characterized by much higher quality with respect to classical US systems.

The data collected by means of an active system, which usually consists of transmitters and/or receivers, can be processed via several algorithms to yield ultrasonic images of the objects of interest (OI). The problem of recovering the features of the objects in the imaging domain is an inverse scattering (IS) problem (Colton and Kress, 2012; Pastorino, 2010).

Solving the acoustic problem in a fast, accurate and robust way is still challenging mainly due to the ill-posedness and non-linearity issues. The first one is responsible for the instability of the solution and is related to the fact that the problem at hand is underdetermined; therefore a small of amount of noise in the data may drive into completely unreliable solutions. Thus, the need of proper regularisation strategies becomes mandatory in order to obtain good recoveries.

On the other hand, the non-linearity of the IS problem increases its difficulty and forces the use of proper minimisation strategies in order to avoid false solutions. Generally, the commonest approach to handle the non-linearity of the IS problem is to employ weak scattering approximations (Pierri et al., 1999; Salucci et al., 2013; Cui et al., 2004; Ambrosanio et al., 2014), which does not handle the ill-posedness issue. However, weak scattering approximations do

[a] https://orcid.org/0000-0002-7608-6686
[b] https://orcid.org/0000-0003-3669-8183
[c] https://orcid.org/0000-0002-5964-8667
[d] https://orcid.org/0000-0002-5403-5482

not consider for important non-linear waves, introducing artifacts and distortions in the solution. Moreover, several applications require the knowledge of the mechanical features of the objects under test, especially in the biomedical framework. For instance, this data might be fundamental as a priori information for hybrid strategies which exploit also electromagnetic features (i.e., microwave imaging) as well as other techniques, which can take advantage of the synergy with ultrasound approaches (Omer et al., 2018).

To this aim, in this paper an ultrasound (US) multiview-multistatic (MV-MS) tomographic imaging system is proposed. The system is a cheap, in-house device which has been designed, built and tested at University of Naples Parthenope. Some qualitative imaging results for an air-based setup are presented as preliminary case study with the perspective of providing a test-bed for biomedical imaging of tissues, e.g. for breast cancer imaging applications, in order to promote pure ultrasound or hybrid microwave and acoustic strategies for achieving clinically effective imaging systems.

This system might support standard medical exams as complementary strategy for early breast cancer diagnosis. This would allow a more frequent screening by overcoming the safety issues related to classical mammography as well as the high costs related to MRI. Last, but not least, the proposed system might overcome some important limitations of standard ultrasound imaging, such as the reliance on the human operator who performs the exam and the poor quality of the images.

In order to evaluate the performance of different inversion approaches, experimental data sets are mandatory. This is the main motivation of this work, where we present an UT system and share the produced data.

2 PRINCIPLES OF ULTRASOUND TOMOGRAPHY

In the field of UT, the main goal is to create quantitative as well as qualitative maps of the morphological and mechanical features of unknown objects located in inaccessible domains. Due to the non-destructive feature of this analysis, it can be performed starting from data collected outside of the imaging domain, which can be of high interest mainly for biomedical applications due to the non-invasive feature of this methodology.

Regarding the collection of data, the object of interest (OI) is surrounded by several US sensors (both transmitters and receivers) which operate in a MV-MS fashion, i.e. one transducer per time is active while all the others record the scattered signal. This procedure continues until all the transducers have acted as transmitters per each frequency in the selected bandwidth. The background medium is usually homogeneous and its mechanical features are chosen in order to maximise the matching with the targets and allow the penetration. A sketch of the simplified two-dimensional (2D) geometry at hand is shown in Fig. 1.

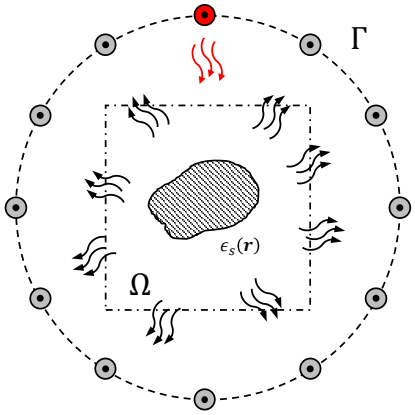

Figure 1: Two-dimensional geometry of the imaging problem. Red circle: active sensor (i.e., transmitter), gray circles: receivers. The unknown object is located in the imaging domain Ω and the sensors are on a measurement curve Γ.

In this framework, two different geometries can be defined. The first one containing the objects of interest, which is known as imaging domain and is denoted as Ω, while the second one contains all the transmitters and receivers and is known as data domain and is denoted as Γ. For practical applications, the data which are acquired in order to provide an estimate of the unknown objects are the scattered field pressure data. In order to obtain them, some measurements without the objects in the imaging domain are performed, also known as incident field measurements. Then, the difference between the pressure field with the objects and the incident field provides the scattered field, which represents the input of the imaging chain.

2.1 Mathematical Formulation

For the considered simplified 2D scenario, the integral equation which governs the scattered field pressure as a function of targets' compressibility, attenuation and density profiles can be written as (Haynes and Moghaddam, 2010; Mojabi and LoVetri, 2015):

$$u_{sct}(\boldsymbol{r}_R,\boldsymbol{r}_T,\omega) =$$
$$= k_b^2 \int_\Omega g(\boldsymbol{r}_R,\boldsymbol{r}',\omega)\cdot\chi_1^c(\boldsymbol{r}',\omega)\cdot u_{tot}(\boldsymbol{r}',\boldsymbol{r}_T,\omega)d\boldsymbol{r}' +$$
$$+ \int_\Omega g(\boldsymbol{r}_R,\boldsymbol{r}',\omega)\nabla\cdot\left[\chi_2(\boldsymbol{r}',\omega)\nabla u_{tot}(\boldsymbol{r}',\boldsymbol{r}_T,\omega)\right]d\boldsymbol{r}'$$
$$\boldsymbol{r}_T,\boldsymbol{r}_R\in\Gamma, \qquad (1)$$

where $g(\boldsymbol{r}_R,\boldsymbol{r}',\omega)$ is the Green's function of the background medium, k_b is the complex background wavenumber and u_{sct} and u_{tot} are the scattered and total pressure fields, and a time-harmonic exponential factor $e^{j\omega t}$ is omitted. Finally, χ_1^c and χ_2 are the contrasts of compressibility and of inverse density respectively, defined as:

$$\chi_1^c(\boldsymbol{r},\omega) = \frac{\kappa(\boldsymbol{r},\omega)-\kappa_b(\omega)}{\kappa_b(\omega)} - j\frac{2\alpha_m(\boldsymbol{r},\omega)}{k_b}, \qquad (2)$$

$$\chi_2(\boldsymbol{r},\omega) = \frac{\rho^{-1}(\boldsymbol{r},\omega)-\rho_b^{-1}(\omega)}{\rho_b^{-1}(\omega)}, \qquad (3)$$

with $\kappa(\boldsymbol{r},\omega)$ compressibility $\rho(\boldsymbol{r},\omega)$ density and $\alpha_m(\boldsymbol{r},\omega)$ attenuation at position $\boldsymbol{r}$ and frequency ω, respectively, while the subscript b stands for the background case.

Imaging approaches aims at finding a stable solution of the inverse scattering problem illustrated in Eq. (1), providing quantitative maps of compressibility, density and attenuation of the objects located in the investigation domain, usually in a nonlinear fashion via iterative methods in order to determine both morphological and mechanical contrast of the targets. However, due to the ill-posedness of the problem at hand, some regularization strategies based on some a priori information are also mandatory to obtain stable solutions.

In addition to these classical approaches, the so-called *qualitative* methods can be of interest, since they only aims at the reconstruction of the morphological features of the scatterers, and usually exploit a linear framework, which avoids the issue of false solutions meantime keeping the computational burden low (Belkebir et al., 1997).

2.2 Imaging Via the Linear Sampling Method

Among the most employed qualitative approaches, the linear sampling method (LSM) seems to be a good candidate to carry out the inversion. It provides an estimate of targets' support via an auxiliary linear problem based on the far-field equation:

$$\int_\Gamma u_{sct}(\boldsymbol{r}_R,\boldsymbol{r}')\xi\left(\boldsymbol{r}_s,\boldsymbol{r}'\right)d\boldsymbol{r}' = g\left(\boldsymbol{r}_R,\boldsymbol{r}_s\right), \qquad (4)$$

with $\boldsymbol{r}_s\in\Omega$ denoting an arbitrary point that samples the region under test, $\boldsymbol{r}_R\in\Gamma$ the curve on which transmitters and receivers are located, and ξ is the unknown function related to target support to be sought (Crocco et al., 2012; Bevacqua and Palmeri, 2019).

The problem shown in Eq. (4) is ill-posed (Colton and Kress, 2012) and thus requires a proper regularisation strategy in order to obtain a stable solution. A well-known, simple and efficient strategy is represented by the Tikhonov regularisation (Tikhonov et al., 2013), which can be applied for the solution of Eq. (4). Then, an estimate of targets' support is obtained by evaluating the L^2-norm of the Herglotz density ξ for every sampling point $\boldsymbol{r}_s\in\Omega$, since this function assumes low values in the targets' support location and diverges in the other points. Thus, it is possible to define the LSM indicator:

$$I\left(\boldsymbol{r}_s\right) = \int_\Gamma \left|\xi\left(\boldsymbol{r}_s,\boldsymbol{r}'\right)\right|^2 d\boldsymbol{r}', \qquad (5)$$

which can be easily evaluated via singular value decomposition.

3 PROTOTYPE OVERVIEW AND IMAGING RESULTS

In this section, the cheap in-house MV-MS UT system designed, built and tested at University of Naples Parthenope is presented. A picture of the prototype is shown in Fig. 2. In order to obtain a spatial diversity of the data, which represents an important requirement for the imaging via MV-MS systems, a rotating platform was located in the centre of the imaging domain. This platform is controlled remotely via a micro-stepper engine, which has an angular precision of one thousandth degree, which allows a good accuracy in the position of the sensors circular array. The region of interest (ROI), i.e. the imaging area in which the objects are located, coincides with the rotating platform, i.e. a circle with a diameter of 28 cm.

The transmitter is connected to a waveform generator (model 33220A manufactured by Agilent Technologies) that produces a cosine signal at 40 kHz. At this operating frequency, the wavelength is approximately 8.5 mm in air background. The transducer radiating pattern is approximately $\pm 30^\circ$ at -6 dB and it is the same both in the vertical as well as horizontal planes. All the sensors, one transmitter and twenty-one receivers, are located on a wooden ring of 17.5-cm radius at a height of 44 cm, and they are equally-spaced on the circle (with an error in their location lower than one fourth of wavelength). A second wooden ring is mounted on the top of the prototype in order to ensure the stiffness of structure.

Figure 2: A picture of the laboratory-developed US imaging system. Sensors (1 Tx, 21 Rx) are located on a wooden ring. The multiview-multistatic configuration is realised via a rotating table the targets are located on, in order to virtually simulate the movement of the sensors ring.

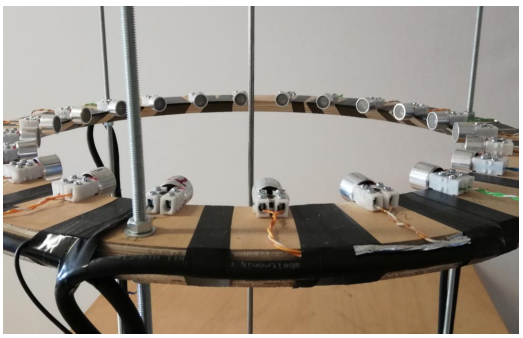

Figure 3: A simple test case with a single metallic cylinder located on the rotating table.

The sensors used as transmitter and receiver are, respectively, 40LT16 and 40LR16 both manufactured by SensComp.

The scattered US waves received by 40LR16 sensors are acquired by PCI-6251 analog-to-digital converters boards manufactured by National Instruments. These boards have a sixteen-bit resolution and a maximum sampling rate of 1.25 MS/s. In the measurement campaign, the sampling frequency was fixed at 100 kHz with sixteen-bit precision. A LabVIEW code was employed to manage the acquisition steps, including the control of ROI rotation. The acquisition protocol consists of a stepped movement and in each position the system stops and acquires for 0.5 second, and then goes on to the next angular position. Once acquired, the signals were pre-processed in Matlab environment. At this step, the signals were filtered in the frequency domain in order to extract only the component at 40 kHz. Subsequently, the the beat signals (amplitude and phase) are measured.

In order to make available several heterogeneous dataset, different scenarios have been implemented. More in detail, objects of different materials (metal, wood, polystyrene) and shapes (circular, rectangular and irregular sections) have been acquired. Within this manuscript, results related to metallic cylinders (4-mm diameter) are reported. A picture of the considered acquisition is shown in Fig 3.

In Fig. 4, the reconstructed sections in case of one (left image) and two (right image) cylinders are reported. It is worth to note that, despite of the high contrast between the mechanical properties of the metal and the air, the shape and the location of the targets are correctly identified, appearing in a ring shape (Fig. 4a). This behaviour in the case of impenetrable objects is in accordance with the literature (Bevacqua and Isernia, 2017), as the mechanical vibrations induced by an external active source in the targets only exist on the boundary of targets support. However, even though the non-linearity of the scenario under test becomes more stressed in the case of two cylinders (Fig. 4b), it is still possible to identify the targets correctly, both in terms of shape and position. future acquisitions related to all the considered scenarios will we uploaded on-line and made available on request.

4 CONCLUSION

In this manuscript, a tomographic in-house ultrasound-based multiview-multistatic imaging system has been designed, built and tested. The performance assessment on cylindrical metallic objects via a classic inversion approach (i.e., the linear sampling method) is reported.

It is worth to underline that the relationship between the scattered field and the object to be retrieved defines a problem that is non-linear and ill-posed. In order to cure this instability, some regularisation strategies are required to avoid unreliable recoveries. From this point of view, the use of multiview data can partially overcome this limitation, especially for noise reduction. Moreover, the use of multi-frequency data could improve considerably the available independent information, allowing better reconstructions, which

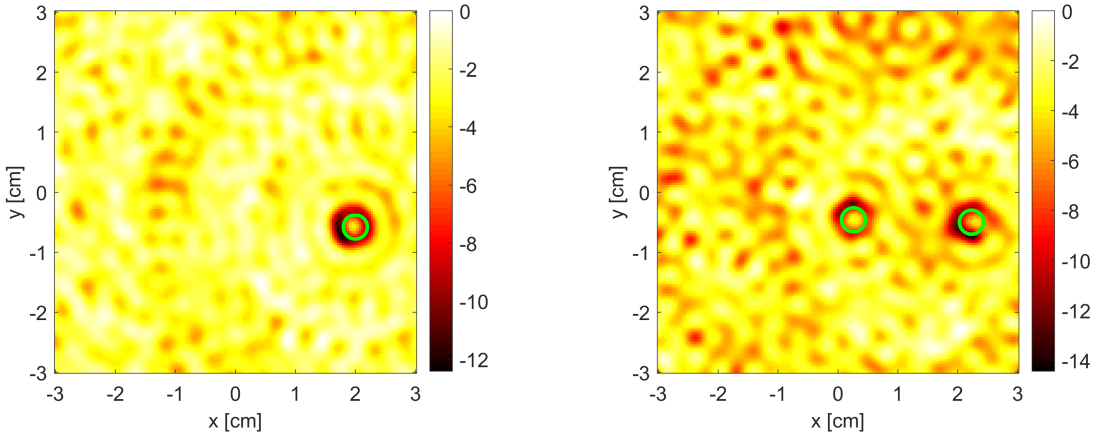

(a) (b)

Figure 4: Imaging results of the data acquired by the proposed prototype via the linear sampling method. (a) single cylinder and (b) two-cylinder reconstructions. The references are the light-green circles.

can be easily implemented by employing proper hardware solutions.

Even though the proposed system is air-coupled and provides a qualitative imaging of targets support, it can be easily generalised to the underwater acoustic imaging case, which represents a convenient, preliminary test before moving to the imaging of human tissues. For instance, in the framework of breast cancer imaging, the use of this kind of systems could be beneficial for early diagnosis, since it is safe and allows a frequent screening which may be a complementary exam to support cancer diagnosis and advancing classic ultrasound.

Future work will focus on the design and building of a water-matched prototype for the performance assessment with breast tissue mimicking phantoms.

REFERENCES

Abdollahi, N., Kurrant, D., Mojabi, P., Omer, M., Fear, E., and LoVetri, J. (2019). Incorporation of ultrasonic prior information for improving quantitative microwave imaging of breast. *IEEE Journal on Multiscale and Multiphysics Computational Techniques*, 4:98–110.

Alqadah, H. F. (2016). A compressive multi-frequency linear sampling method for underwater acoustic imaging. *IEEE Transactions on Image Processing*, 25(6):2444–2455.

Ambrosanio, M., Autieri, R., and Pascazio, V. (2014). A compressive sensing based approach for microwave tomography and gpr applications. In *2014 IEEE Geoscience and Remote Sensing Symposium*, pages 3144–3147. IEEE.

Belkebir, K., Kleinman, R. E., and Pichot, C. (1997). Microwave imaging-location and shape reconstruction from multifrequency scattering data. *IEEE Transactions on Microwave Theory and Techniques*, 45(4):469–476.

Bevacqua, M. T. and Isernia, T. (2017). Shape reconstruction via equivalence principles, constrained inverse source problems and sparsity promotion. *Progress In Electromagnetics Research*, 158:37–48.

Bevacqua, M. T. and Palmeri, R. (2019). Qualitative methods for the inverse obstacle problem: A comparison of experimental data. *Journal of Imaging*, 5(4):47.

Colton, D. and Kress, R. (2012). *Inverse acoustic and electromagnetic scattering theory*, volume 93. Springer Science & Business Media.

Crocco, L., Di Donato, L., Catapano, I., and Isernia, T. (2012). An improved simple method for imaging the shape of complex targets. *IEEE Transactions on Antennas and Propagation*, 61(2):843–851.

Cui, T. J., Qin, Y., Wang, G.-L., and Chew, W. C. (2004). Low-frequency detection of two-dimensional buried objects using high-order extended born approximations. *Inverse Problems*, 20(6):S41.

Haynes, M. and Moghaddam, M. (2010). Large-domain, low-contrast acoustic inverse scattering for ultrasound breast imaging. *IEEE Transactions on Biomedical Engineering*, 57(11):2712–2722.

Mojabi, P. and LoVetri, J. (2015). Ultrasound tomography for simultaneous reconstruction of acoustic density, attenuation, and compressibility profiles. *The Journal of the Acoustical Society of America*, 137(4):1813–1825.

Mojabi, P. and LoVetri, J. (2017). Evaluation of balanced ultrasound breast imaging under three density profile assumptions. *IEEE Transactions on Computational Imaging*, 3(4):864–875.

Omer, M., Mojabi, P., Kurrant, D., LoVetri, J., and Fear, E. (2018). Proof-of-concept of the incorporation of ultrasound-derived structural information into microwave radar imaging. *IEEE Journal on Multiscale and Multiphysics Computational Techniques*, 3:129–139.

Pastorino, M. (2010). *Microwave imaging*, volume 208. John Wiley & Sons.

Pierri, R., Persico, R., and Bernini, R. (1999). Information content of the born field scattered by an embedded slab: multifrequency, multiview, and multifrequency–multiview cases. *JOSA A*, 16(10):2392–2399.

Salucci, M., Sartori, D., Anselmi, N., Randazzo, A., Oliveri, G., and Massa, A. (2013). Imaging buried objects within the second-order born approximation through a multiresolution-regularized inexact-newton method. In *2013 International Symposium on Electromagnetic Theory*, pages 116–118. IEEE.

Tikhonov, A. N., Goncharsky, A., Stepanov, V., and Yagola, A. G. (2013). *Numerical methods for the solution of ill-posed problems*, volume 328. Springer Science & Business Media.